



Turbulent Black Holes

Huan Yang,^{1,2} Aaron Zimmerman,³ and Luis Lehner¹

¹*Perimeter Institute for Theoretical Physics, Waterloo, Ontario N2L2Y5, Canada*

²*Institute for Quantum Computing, University of Waterloo, Waterloo, Ontario N2L3G1, Canada*

³*Canadian Institute for Theoretical Astrophysics, 60 St. George Street, Toronto, Ontario M5S3H8, Canada*

(Received 17 October 2014; revised manuscript received 10 January 2015; published 23 February 2015)

We demonstrate that rapidly spinning black holes can display a new type of nonlinear parametric instability—which is triggered above a certain perturbation amplitude threshold—akin to the onset of turbulence, with possibly observable consequences. This instability transfers from higher temporal and azimuthal spatial frequencies to lower frequencies—a phenomenon reminiscent of the inverse cascade displayed by $(2 + 1)$ -dimensional fluids. Our finding provides evidence for the onset of transitory turbulence in astrophysical black holes and predicts observable signatures in black hole binaries with high spins. Furthermore, it gives a gravitational description of this behavior which, through the fluid-gravity duality, can potentially shed new light on the remarkable phenomena of turbulence in fluids.

DOI: [10.1103/PhysRevLett.114.081101](https://doi.org/10.1103/PhysRevLett.114.081101)

PACS numbers: 04.70.Bw, 04.30.Nk, 47.27.Ak

Black holes are fascinating objects. They play a fundamental role in a plethora of energetic phenomena in our Universe—for example, as the engines of active galactic nuclei, x-ray binaries, and possibly even as regulators of galactic structure. In addition, they have become central tools in the study of field theories through the framework of holography [1]. This includes attempts to understand superfluidity, superconductivity, and quark-gluon plasmas obtained in energetic collisions (see, e.g., Refs. [2–4]). One particularly exciting connection inspired by holography is the “fluid-gravity” duality, which indicates the dynamics of black holes in asymptotically anti-de Sitter (AAdS) spacetimes in $(d + 1)$ dimensions can be mapped to the physics described by conformal fluids governed by viscous, relativistic hydrodynamics in d dimensions [5,6]. This opens the door to search on one side of the duality for particular behavior known to exist on the other. For instance, this duality has motivated studies showing that particular gravitational scenarios can become turbulent when their fluid counterparts have high Reynolds numbers [7–9]. Additionally, concepts in hydrodynamics, such as *entropy*, have geometric counterparts related to curvature quantities [7]. This duality can also shed light on poorly understood phenomena from a new perspective. Analyzing turbulence from an intrinsically gravitational point of view is thus an exciting prospect.

In this Letter, we develop a method to do precisely this and consider realistic, asymptotically flat black holes. Our analysis describes how a parametric instability mimics the properties of the onset of turbulence—which does not require the “confining properties” of asymptotically AdS spacetimes—and motivates the definition of a gravitational Reynolds number. We first review general properties of turbulent flows, salient features of the fluid-gravity duality, and parametric instability.

Hydrodynamic turbulence.—Turbulence is a ubiquitous property of fluid flows with sufficiently high Reynolds

number ($\text{Re} \equiv \rho/\eta v\lambda \gg 1$) [10,11]. Here v and λ refer to the typical velocity and wavelength of characteristic modes of the solution, and ρ, η the fluid density and viscosity. At high Re , nonlinear interactions prevail over dissipation due to viscosity, and chaotic behavior ensues. Turbulence displays several features: (i) an cascade (which can be toward higher frequencies in 3-spatial dimensions or lower ones in 2-spatial dimensions), (ii) an exponential growth—possibly transitory—of additional modes in the solution, and (iii) a breaking of initial symmetries of the flow, which are only recovered in a statistical sense at later times. Furthermore, in the absence of a driving force, global norms of the solution display a transient power-law decay, and viscous losses then decrease Re until turbulence ends. Beyond these broad aspects, a full understanding of turbulence is missing. A promising new road of study has been furnished through the fluid-gravity duality, provided a purely gravitational model for turbulence is available. Here we present a step toward understanding the onset of gravitational turbulence and uncover possible astrophysical consequences.

Fluid-gravity duality and black holes in AAdS vs asymptotically flat spacetimes.—The fluid-gravity duality indicates that long-wavelength perturbations of black holes in AAdS spacetimes can be described by relativistic hydrodynamic equations (with an equation of state given by $p = \rho/d$) [6]. In addition to connecting known hydrodynamic and gravitational effects, such as loss of energy through the black hole horizon to viscous dissipation, the duality can reveal new phenomena. The presence of turbulence in hydrodynamics indicates that a similar behavior appears in perturbed AAdS black holes, and this expectation has been confirmed by simulations of the gravitational side of the problem [8] which are direct counterparts of those in the hydrodynamical front [7,9]. Nevertheless, an analytical understanding of what mediates turbulence in gravity is an open question, as well as whether such striking behavior can take place in the realistic case of asymptotically flat (AF) spacetimes.

In considering these questions, we recall the differences in how these two classes of spacetimes relate to hydrodynamics. Regardless of the class considered, a gradient expansion of the Einstein equations for long-wavelength perturbations of black holes gives rise to relativistic hydrodynamic equations on a timelike hypersurface [12,13]. However, only AAdS has a unique surface, lying at infinity, where the correspondence can be defined unambiguously. In both classes, perturbed black holes have a spectrum of free, damped oscillation modes known as quasinormal modes (QNMs; see, e.g., Refs. [14,15]). Black holes in AAdS only lose energy through the event horizon (as its boundary acts as a confining box), while energy in AF spacetimes can also be lost to infinity. Consequently, QNMs decay considerably more slowly in the AAdS case. From the hydrodynamic view, a slow decay of QNMs implies low viscosity and a possibly higher Reynolds number [9]. This motivates us to study interactions between QNMs in rapidly spinning black holes—which have a slowly decaying family of such modes—and, in particular, how the signature of turbulence might arise in the AF case. By doing so, we provide a gravitational description of the onset of turbulence in realistic black hole spacetimes.

Damped parametric oscillator.—The parametric instability in black holes described below is analogous to the simple parametric oscillator. A parametrically driven oscillator can be described by the equation

$$\ddot{q} + \gamma\dot{q} + \omega^2[1 + 2f(t)]q = 0, \quad (1)$$

where ω is the intrinsic harmonic frequency, γ is a weak damping coefficient ($\gamma \ll \omega$), and $f(t)$ characterizes the parametric driving. The solution to this equation is bounded in time, except when $f(t)$ oscillates at approximately twice the intrinsic frequency: $f(t) = f_0 \cos \omega' t$, $\omega' \approx 2\omega$. In this case the time dependence of the solution is described by $e^{\Omega t}$, with the rate $2\Omega \approx \omega \sqrt{f_0^2 - \omega^{-4}[\omega^2 - (\omega'/2)^2]^2} - \gamma$. When ω' is close to 2ω , a small parametric driving amplitude f_0 will be able to excite a growing solution, which is referred to as a parametric instability. For a given value of the damping coefficient γ , there is a critical relation that f_0 and ω satisfy at the separatrix between growth or decay. This is related to the critical gravitational Reynolds number for the onset of turbulent behavior in perturbed black holes.

Perturbed black holes in AF scenarios and turbulence.—In four dimensions, a stationary AF black hole is characterized by its mass M and spin parameter a , which has a maximum value of $a/M = 1$. When $a/M \approx 1$ or $\epsilon \equiv 1 - a/M \ll 1$, there exists a family of quasinormal modes with a small damping rate proportional to $\sqrt{\epsilon}$ (referred as zero-damping modes or ZDMs) [16–19]. These modes have time dependence $e^{i\omega_{lmn}t}$, with

$$\omega_{lmn} \equiv \omega_R - i\omega_I \approx \frac{m}{2} - \frac{\delta\sqrt{\epsilon}}{\sqrt{2}} - i\left(n + \frac{1}{2}\right) \frac{\sqrt{\epsilon}}{\sqrt{2}}, \quad (2)$$

(with l, m, n denoting the angular, azimuthal, and overtone numbers, respectively, and δ a function of l, m

and the spin-weight of the perturbation considered; see the Supplemental Material [20]). Consider as an example a black hole perturbed by a small mass falling toward the event horizon. This excites some of the ZDMs to a characteristic amplitude h_0 . Once a particular ZDM is excited, at linear order its amplitude decays exponentially with a rate $\propto \sqrt{\epsilon}$ (in hydrodynamical terms, this decay corresponds to laminar flow). However, nonlinear coupling between modes introduces a competing transfer between modes at a rate dependent on h_0 . As we decrease ϵ , the mode-mode coupling mechanism may overcome decay, even pumping up modes that are not initially excited, regardless of how weak the initial perturbation is. This is analogous to the onset of turbulence at high Re.

Formalism.—As we go beyond linear perturbation theory, the spacetime metric g can be expanded as $g = g_B + h^{(1)} + h^{(2)} + \dots$, where g_B is the background Kerr metric and $h^{(n)}$ is the n th order perturbation. We are interested in how an initial ZDM metric perturbation $h^{(1)}$ might trigger other modes through parametric resonance. One way to analyze the problem is to take $g_{\bar{B}} = g_B + h^{(1)}$ as a dynamical background metric and study the evolution of $h^{(2)}$ on it. To avoid delicate gauge issues for the higher order metric perturbations, we adopt a simpler version of this approach, solving the evolution of a massless scalar field in the dynamical background $g_{\bar{B}}$. This field obeys the wave equation

$$\square_{\bar{B}}\Phi = 0, \quad (3)$$

and we bear in mind that Φ plays a role analogous to $h^{(2)}$. Since $\square_{\bar{B}}\Phi$ is gauge invariant, our results concerning the parametric instability are gauge invariant.

The first-order perturbation $h^{(1)}$ corresponding to a quasinormal mode with index (l, m, n) is

$$h_{\mu\nu}^{(1)} = 2h_0 \Re[Z_{\mu\nu}(r, \theta)e^{-i\omega t + im\phi}], \quad (4)$$

where $h_0(t) = h_0 e^{-\omega_I t}$. As we perturb the background metric g_B to $g_B + h^{(1)}$, Φ obeys

$$\square_{\bar{B}}\Phi \approx \left[\square_B + \frac{1}{\Sigma} \mathcal{H}(h^{(1)}) \right] \Phi. \quad (5)$$

Here $\Sigma \equiv r^2 + a^2 \cos^2 \theta$ and $\mathcal{H}(\cdot)$ is a time-dependent operator linear in its argument. The time dependence of \mathcal{H} is crucial in triggering the parametric instability, which occurs when the temporal and azimuthal frequencies of the parent $h^{(1)}$ match the daughter mode Φ . For rapidly spinning Kerr black holes, this occurs when the daughter mode satisfies $m' = m/2$, as Eq. (2) guarantees that $\omega'_R \approx \omega_R/2$ as well. We make the ansatz

$$\Phi_{l'm'n'}(x^\mu) = [g_j(t)e^{(-1)^j i\omega_R/2t - (-1)^j im'\phi} Y_{l'm'n'}] e^{-\omega'_I t},$$

(summing over $j = 1, 2$), with g_1, g_2 characterizing the time dependence and $Y_{l'm'n'}(r, \theta)$ the perturbed wave function. The equations of motion determining g_1, g_2 are closely related to the parametric instability previously

discussed. The solution to these equations is given by $g_j = A_j e^{\int \alpha(t') dt'}$ with

$$\alpha = \pm \sqrt{|Hh_0(t)/Qm'|^2 - (\omega'_R - \omega_R/2)^2}, \quad (6)$$

where H has the physical meaning of mode-mode coupling strength and Q gives the susceptibility of the wave equation to a perturbation of the mode frequency [20]. At leading order, Q is independent of m . An exponential growth in Φ will occur if $\Omega \equiv \alpha(t) - \omega'_l > 0$, i.e., when

$$h_0(t)/(m'\omega'_l) - |Q/H| \sqrt{(\omega'_R - \omega_R/2)^2/\omega_l'^2 + 1} > 0. \quad (7)$$

We emphasize that given $m' = m/2$, both $\omega'_R - \omega_R/2$ and ω'_l can be read off from Eq. (2), and both are $\propto \sqrt{\epsilon}$. We choose to normalize the radial wave function of the ZDMs such that $|H/Q|$ is ϵ independent—in other words, the effect of mode-mode coupling stays constant for varying black hole spins [38]. These properties are useful in defining and interpreting the gravitational Reynolds number.

Turbulent black holes.—Based on the above analysis, consider an initial ZDM mode with $m = 2m'$ and amplitude h_0 ; as we increase h_0 , all the secondary ZDMs with azimuthal quantum number m' satisfying Eq. (7) are parametrically excited. As these daughter modes grow, energy flows from the parent mode to the daughter modes, and the parent mode experiences back reaction due to the mode coupling. Ignoring this backreaction, these secondary modes grow as long as Eq. (7) holds, but in a realistic situation, parametric growth terminates when the amplitudes of the parent mode and the secondary modes become comparable requiring a fully nonlinear treatment (or numerical study, e.g., Ref. [39]). The gravitational parametric instability displays an inverse cascade, as flows from modes with high azimuthal frequencies to modes with lower azimuthal frequencies, and from higher to lower temporal frequencies. An initial azimuthal mode m generates a series of modes with azimuthal number $m/2^p$ after p generations. This is similar to the inverse cascade in $(2+1)$ -dimensional turbulent fluids. Since modes with the same m' but high l can also be excited, there is also a direct transfer of toward higher overall angular frequencies.

From the criteria in Eq. (7), we define a gravitational Reynolds number Re_g , taking $m = 2m'$, and with ω'_l

chosen to be the lowest possible decay rate of all the ZDMs, $\gamma_\eta = \sqrt{\epsilon/8}$. This gives

$$\text{Re}_g \equiv h_0/(m\gamma_\eta). \quad (8)$$

For a mode having Re_g below some critical value given in Eq. (7), no growth is expected, and the mode behaves in a “laminar” manner, decaying normally. For larger values of Re_g , turbulent behavior ensues, driving growing modes and a richer angular structure. Once Re_g decreases below the critical value for a given mode, that mode again decays exponentially. Notice that the natural identifications among hydrodynamical quantities {ratio of viscosity to density, perturbation wavelength, and velocity} and gravitational ones {lowest QNM decay rate, inverse of azimuthal number of the perturbation, and amplitude of perturbation} respectively as, $\{\eta/\rho \leftrightarrow \gamma_\eta, \lambda \leftrightarrow 1/m, v \leftrightarrow h_0\}$ gives $\text{Re}_g \leftrightarrow \text{Re}$. Our definition arises from the criteria for the onset of instability, and it agrees with the one proposed in Ref. [9] motivated through the fluid-gravity duality. Table I presents a list of numerical values of the critical Re_g , beyond which the parametric instability for different driving and secondary modes will be turned on. We consider only the lowest overtone modes, $n = n' = 0$. We can see that for fixed ϵ and m , the critical Re_g asymptotes to a constant value for high l modes. One may argue that this means modes with arbitrarily high l are all excited. However, as discussed in Yang *et al.* [18,19] there is a minimum, critical ϵ , beyond which the required phase-matching condition gradually fails to hold. A conservative estimate for this critical value is $\epsilon_c \propto l^{-2}$. So for a given spin, there is a high angular frequency cutoff scale where the instability criteria is not satisfied and the transfer stops.

Figure 1 illustrates the rich angular structure of the perturbed spacetime that arises due to the parametric instability, due to driving by the fundamental $l = 2$, $m = 2$, $n = 0$ QNM. We take for our fiducial example $\epsilon = 2 \times 10^{-3}$ ($a/M = 0.998$) [40] and $h_0(t=0) = (1/8)\sqrt{\epsilon}$. This amplitude is motivated by the expected excitation following a large mass-ratio inspiral, such as can occur in supermassive binary black hole coalescence following galaxy mergers [20]. Note that for such an h_0 the criteria for growth is independent of spin, so long as $\epsilon \ll 1$. In the fully gravitational case, we can expect a similar development of structure in both the far-field radiation and

TABLE I. Critical Re_g for different parent daughter modes with $m = 2m'$. These numbers are obtained in the ingoing radiation gauge using a value for $|H/Q|$ evaluated at $\epsilon = 10^{-5}$ (although they are expected to be ϵ independent, numerically we use a small ϵ to reduce systematic error in the wave functions); extrapolation to lower spins and error in the matching of radial eigenfunctions are the dominant sources of error, which we estimate conservatively to be 10%. The parent mode of the $42 \rightarrow 11$ driving has an imaginary value of δ , whereas the parents in the other two cases have real δ , which may explain the large critical Reynolds numbers in those cases. Note also that the $44 \rightarrow 22$ driving is unique in the sense that both its parent and daughter mode have real δ .

(l, m)	$l' = 1$	$l' = 2$	$l' = 3$	$l' = 4$	$l' = 5$	$l' = 6$	$l' = 7$	$l' = 8$
(2, 2)	0.287	0.163	0.130	0.122	0.117	0.115	0.113	0.111
(4, 2)	43.2	62.1	92.7	123	118	118	117	117
(4, 4)		3.62	0.00676	0.0114	0.0108	0.0104	0.0101	0.0100

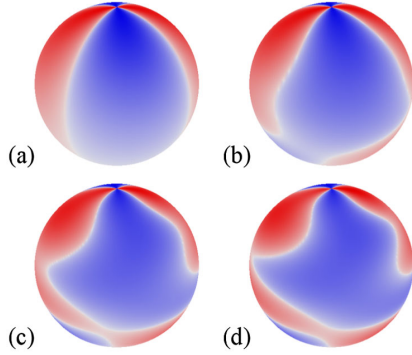


FIG. 1 (color online). Snapshots of parametrically driven modes on a sphere of constant radius. We plot the dominant $(2, 2)$ spin $s = -2$ spheroidal harmonic from a collective driving mode, plus the spin-0 $(l, 1)$ spheroidal harmonics for all of the growing scalar modes. Initially $h_0(t=0) = (1/8)\sqrt{\epsilon}$, and $\epsilon = 2 \times 10^{-3}$ ($a = 0.998$). In this case, modes with $2 \leq l \leq 6$ are resonantly excited, with the higher l modes growing faster; the $l > 6$ modes are not ZDMs for this a . At $t/M = 0$, the scalar modes are seeded with equal amplitude 10% of the gravitational mode, and random phases. (a) Reference spin $s = -2$, $(2, 2)$ spheroidal harmonic. (b) At time $t/M = 0$, the seed modes are visible only where the gravitational mode is weak. (c) At time $t/M = 16$, more angular structure has developed. (d) The harmonics at $t/M = 32$ when the amplitude of the $(6, 1)$ scalar mode is closest to the $(2, 2)$ mode.

curvature quantities on the event horizon. Figure 2 shows the amplitudes of the driving gravitational mode and excited scalar modes for the same fiducial example as in Fig. 1. Though we focus on driving by the dominant $(2, 2)$ mode, Table I indicates that modes can be driven by a $(4, 4)$ mode for even smaller values of h_0 .

During the inverse cascade, modes with frequencies 2^{-p} ($p \in \mathbb{Z}$) times the parent mode frequency are excited by parametric resonance. However, in a fully turbulent fluid, transfers throughout the entire spectrum. One possible mechanism for this in the gravitational case is through resonant excitation of additional modes, as occurs in systems of coupled oscillators. For example, two oscillators with frequencies ω_1 and ω_2 , and amplitudes $A_1(t)$ and $A_2(t)$ can drive modes with frequencies $\omega' = \omega_1 \pm \omega_2$, resulting in amplitudes proportional to $A_1 A_2$. These three-mode interactions may not be as strong as the parametric resonance in this specific setup, but they can redistribute later on to both higher and lower frequencies, and fill in the gaps in the spectrum.

Observational consequences.—The parametric instability discussed here focuses on rapidly spinning black holes, where the QNMs decay slowly [41]. Theoretical models arguing for such scenarios have been developed [42,43] and, crucially, there is observational evidence for highly spinning black holes [44,45]. The turbulent instability has several possible signatures [46]. (1) Gravitational wave structure: the turbulent behavior described can have an impact on gravitational wave observations from large mass-ratio mergers involving a rapidly spinning black hole. Such scenarios can arise, for instance, in the inspiral of

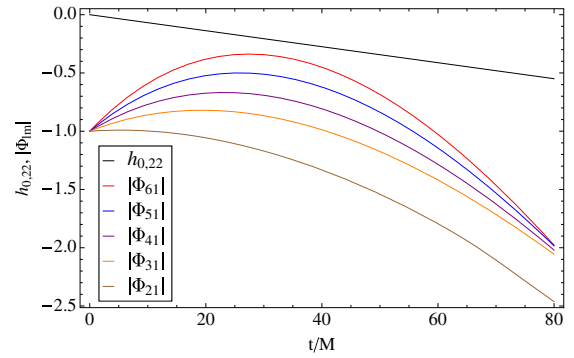


FIG. 2 (color online). Growth of the scalar quasinormal mode amplitudes due to a $(2, 2)$ perturbation, on a logarithmic scale, using the same parameters as in Fig. 1. After initial parametric growth, the driving of each mode turns off as $h_0(t)$ decays, after which the scalar mode decays at its standard exponential rate, which is larger for modes with larger l .

supermassive binary black holes following galaxy mergers. After merger, the final black hole rings down by emitting gravitational waves primarily through the $(2, 2)$ mode. The magnitude of the initial perturbation h_0 is proportional to the mass ratio, and so for smaller μ values Eq. (7) is not satisfied, and distant observers should see mainly the $(2, 2)$ mode during the entire ringdown. However, if the initial perturbation is strong enough, modes with $m = 1$ will be parametrically excited. The growth of the modes can allow them to overtake the amplitude of the $(2, 2)$ mode, in which case a treatment of the back reaction is needed. However, it is possible that a distant observer could measure a growing amplitude of some modes during the ringdown, a clear evidence of the instability, perhaps followed by complicated and turbulent behavior in the mode structure of the observed signal. Gravitational wave signals from supermassive binary black hole mergers would be detectable by pulsar timing arrays (e.g., Ref. [47]) while stellar mass systems are the target of the LIGO, VIRGO, and KAGRA Collaborations [48–50]. (2) Jitter in the black hole geometry: the phenomena discussed indicates that the geometry of the spacetime around a black hole can acquire a rich multipolar structure as a result of an object falling into a rapidly spinning black hole. This structure will impact the surrounding region and, in particular, may cause angular time-dependent shifts in the location of the inner most stable circular orbit. The fractional impact on the inner disk structure would be within an order of magnitude of $h_0(t)$ ($\sim 0.5\%$ for our fiducial model), with a corresponding impact on the emission lines of the accreting material. Such variations would have a unique time signature, and be measurable to the same accuracy as fractional changes in the spin of the black hole (see, e.g., Ref. [51] for an analysis of what is feasible with very large base interferometry).

We thank Stephen Green and Scott Hughes for discussions, and Zachary Mark for his help in a separate study in validating the inner product used here. We also thank

Eric Poisson for valuable comments on this manuscript. We thank Chris Thompson for discussion which led us to identify an error in an earlier preprint. This work was supported by NSERC through Discovery Grants and CIFAR (to L.L.). This research was supported in part by Perimeter Institute for Theoretical Physics. Research at Perimeter Institute is supported by the Government of Canada through Industry Canada and by the Province of Ontario through the Ministry of Research and Innovation.

-
- [1] J. Maldacena, *Int. J. Theor. Phys.* **38**, 1113 (1998).
- [2] P. M. Chesler, H. Liu, and A. Adams, *Science* **341**, 368 (2013).
- [3] G. T. Horowitz, *Lect. Notes Phys.* **828**, 313 (2011).
- [4] J. Casalderrey-Solana, H. Liu, D. Mateos, K. Rajagopal, and U. A. Wiedemann, *Gauge/String Duality, Hot QCD and Heavy Ion Collisions* (Cambridge University Press, Cambridge, UK, 2014).
- [5] G. Policastro, D. T. Son, and A. O. Starinets, *J. High Energy Phys.* **09** (2002) 043.
- [6] S. Bhattacharyya, V. E. Hubeny, S. Minwalla, and M. Rangamani, *J. High Energy Phys.* **02** (2008) 045.
- [7] F. Carrasco, L. Lehner, R. C. Myers, O. Reula, and A. Singh, *Phys. Rev. D* **86**, 126006 (2012).
- [8] A. Adams, P. M. Chesler, and H. Liu, *Phys. Rev. Lett.* **112**, 151602 (2014).
- [9] S. R. Green, F. Carrasco, and L. Lehner, *Phys. Rev. X* **4**, 011001 (2014).
- [10] L. D. Landau and E. M. Lifshitz, *Fluid Mechanics* (Pergamon Press, Oxford, 1987).
- [11] G. Boffetta and R. E. Ecke, *Annu. Rev. Fluid Mech.* **44**, 427 (2012).
- [12] K. S. Thorne, R. H. Price, and D. A. MacDonald, *Black Holes: The Membrane Paradigm* (Yale Univ. Pr., New Haven, USA, 1986).
- [13] R. Emparan, T. Harmark, V. Niarchos, and N. A. Obers, *J. High Energy Phys.* **3** (2010) 063.
- [14] K. Kokkotas and B. Schmidt, *Living Rev. Relativity* **2**, 2 (1999).
- [15] E. Berti, V. Cardoso, and A. O. Starinets, *Classical Quantum Gravity* **26**, 163001 (2009).
- [16] S. Detweiler, *Proc. R. Soc. A* **352**, 381 (1977).
- [17] S. Hod, *Phys. Rev. D* **78**, 084035 (2008).
- [18] H. Yang, F. Zhang, A. Zimmerman, D. Nichols, E. Berti, and Y. Chen, *Phys. Rev. D* **87**, 041502 (2013).
- [19] H. Yang, A. Zimmerman, A. Zenginoğlu, F. Zhang, E. Berti, and Y. Chen, *Phys. Rev. D* **88**, 044047 (2013).
- [20] See Supplemental Material at <http://link.aps.org/supplemental/10.1103/PhysRevLett.114.081101> for perturbative calculations carried out, which includes Refs. [21–37], for details.
- [21] S. A. Teukolsky, *Astrophys. J.* **185**, 635 (1973).
- [22] E. Leaver, *Proc. R. Soc. A* **402**, 285 (1985).
- [23] P. Chrzanowski, *Phys. Rev. D* **11**, 2042 (1975).
- [24] R. M. Wald, *Phys. Rev. Lett.* **41**, 203 (1978).
- [25] C. O. Lousto and B. F. Whiting, *Phys. Rev. D* **66**, 024026 (2002).
- [26] A. Ori, *Phys. Rev. D* **67**, 124010 (2003).
- [27] T. S. Keidl, J. L. Friedman, and A. G. Wiseman, *Phys. Rev. D* **75**, 124009 (2007).
- [28] T. S. Keidl, A. G. Shah, J. L. Friedman, D.-H. Kim, and L. R. Price, *Phys. Rev. D* **82**, 124012 (2010).
- [29] D. A. Nichols, A. Zimmerman, Y. Chen, G. Lovelace, K. D. Matthews, R. Owen, F. Zhang, and K. S. Thorne, *Phys. Rev. D* **86**, 104028 (2012).
- [30] E. Newman and R. Penrose, *J. Math. Phys. (N.Y.)* **3**, 566 (1962).
- [31] S. Chandrasekhar, *The Mathematical Theory of Black Holes* (Clarendon Press, Oxford, 1983).
- [32] E. W. Leaver, *Phys. Rev. D* **34**, 384 (1986).
- [33] S. A. Teukolsky and W. H. Press, *Astrophys. J.* **193**, 443 (1974).
- [34] A. Zenginoğlu and G. Khanna, *Phys. Rev. X* **1**, 021017 (2011).
- [35] K. Glampedakis and N. Andersson, *Phys. Rev. D* **64**, 104021 (2001).
- [36] E. Harms, S. Bernuzzi, and B. Brügmann, *Classical Quantum Gravity* **30**, 115013 (2013).
- [37] A. Porfyriadis and A. Strominger, *Phys. Rev. D* **90**, 044038 (2014).
- [38] This normalization means that the amplitude h_0 of a particular mode excited by a physical process will have an additional dependence on ϵ [20].
- [39] W. E. East, F. M. Ramazanoğlu, and F. Pretorius, *Phys. Rev. D* **89**, 061503 (2014).
- [40] Note that our perturbative analysis is about an isolated black hole, and so a corresponds to the spin parameter of the final black hole in the case of a binary merger.
- [41] This instability for nearly extremal black holes likely relates to the linear and nonlinear horizon instabilities discovered in extremal black holes. See, e.g., S. Aretakis, [arXiv:1206.6598](https://arxiv.org/abs/1206.6598); S. Aretakis, *Phys. Rev. D* **87**, 084052 (2013); and K. Murata, H. S. Reall, and N. Tanahashi, *Classical Quantum Gravity* **30**, 235007 (2013). However, this connection requires further investigation. Note that a similar analysis can be applied to slowly decaying QNMs in other spacetimes, such as Reissner-Nordstrom-anti-de Sitter spacetimes; See, e.g., B. Wang, C. Lin, and C. Molina, *Phys. Rev. D* **70**, 064025 (2004); and E. Berti and K. D. Kokkotas, *Phys. Rev. D* **67**, 064020 (2003). Further analysis for more general spacetimes will be presented elsewhere.
- [42] K. S. Thorne, *Astrophys. J.* **191**, 507 (1974).
- [43] M. Kesden, G. Lockhart, and E. S. Phinney, *Phys. Rev. D* **82**, 124045 (2010).
- [44] J. E. McClintock, R. Narayan, S. W. Davis, L. Gou, A. Kulkarni, J. A. Orosz, R. F. Penna, R. A. Remillard, and J. F. Steiner, *Classical Quantum Gravity* **28**, 114009 (2011).
- [45] G. Risaliti *et al.*, *Nature (London)* **494**, 449 (2013).
- [46] Note that the calculation is performed using analytical QNM frequencies and wave functions in the near extremal limit, and therefore extra caution might be required when dealing with black holes rotating less rapidly.
- [47] R. N. Manchester (International Pulsar Timing Array), *Classical Quantum Gravity* **30**, 224010 (2013).
- [48] B. P. Abbott *et al.* (LIGO Scientific Collaboration), *Rep. Prog. Phys.* **72**, 076901 (2009).
- [49] T. Accadia *et al.* (VIRGO collaboration) *Classical Quantum Gravity* **28**, 114002 (2011).
- [50] K. Somiya (KAGRA Collaboration), *Classical Quantum Gravity* **29**, 124007 (2012).
- [51] A. E. Broderick, T. Johannsen, A. Loeb, and D. Psaltis, *Astrophys. J.* **784**, 7 (2014).